

# Velocity measurements in a ship airwake with crosswind

Cody J. Brownell<sup>1</sup>, Luksa Luznik<sup>2</sup>, Murray R. Snyder<sup>3</sup>, and Hyung-Suk Kang<sup>4</sup>  
*United States Naval Academy, Annapolis, MD 21402*

**In situ air velocity measurements in the near wake of a Navy training ship are presented for an inflow of 15° to starboard. This data is required for the validation of ship airwake simulations, which are used to determine the launch and recovery envelopes for shipborne rotorcraft and for use in piloted flight simulations. The measurements are taken primarily above an aft flight deck, which sits immediately behind a step-like hangar structure. A description of the mean flow structure is included, as well as the Reynolds stresses at numerous points along the ship centerline. Comparisons are made between the present 15° case and the case of a direct headwind, presented previously. Compared to the 0° inflow condition, the flow symmetry is clearly broken with a cross-wind. The port and starboard sides of the deck have very different mean flow profiles and turbulent stress components. An updraft is visible over much of the starboard side of the flight deck, which is not found on the port side, or on either side under a headwind. Along the centerline, the streamwise normal component of the turbulent stresses are much larger in the cross-wind case than in the headwind case, while the shear components have similar magnitudes. This suggests that the wake turbulence is similar, but that in the cross-wind case the flight deck is more heavily burdened by inflow fluctuations from the atmosphere.**

## Nomenclature

$H$	=	step height of hangar immediately forward of flight deck, approx 1.5-m.
$R_{uu}$	=	normal, streamwise Reynolds stress component
$R_{uw}$	=	Reynolds shear stress component
$U_\infty$	=	mean velocity in the horizontal plane, measured from above the ship bow
$\rho_{ij}$	=	two-point cross-correlation function
YP	=	Navy training vessel, 108-ft long.
$u, v, w$	=	velocity components in the x, y, and z directions, respectively
$x$	=	coordinate along the length of ship, with origin at the hangar face, positive aft
$y$	=	cross-ship coordinate, origin at the ship center, positive starboard
$z$	=	vertical coordinate, origin at the flight deck surface, positive up

## I. Introduction

**R**OTORCRAFT operating in a marine environment must interface with a pitching, plunging, rolling flight deck, while subject to turbulence from both the atmosphere and from the wake created by airflow over the upstream ship superstructure. At present, launch and recovery envelopes for rotorcraft are determined from trials at sea, which require a significant time commitment and cooperation from the weather. Validated, real-time simulations of the airflow over naval vessels would facilitate the determination of safe operating envelopes, greatly reducing both cost and pilot risk.<sup>1-3</sup>

The simulation of the airwake from a ship superstructure is challenging because of a number of factors.<sup>4</sup> Reynolds numbers based on ship length can be  $10^9$  or higher, meaning the range of relevant length scales is

---

<sup>1</sup> Assistant Professor, Mechanical Engineering Department, 590 Holloway Rd 11/C, Annapolis, MD 21402, AIAA Member.

<sup>2</sup> Assistant Professor, Mechanical Engineering Department, 590 Holloway Rd 11/C, Annapolis, MD 21402.

<sup>3</sup> Permanent Military Professor, Mechanical Engineering Department, 590 Holloway Rd 11/C, Annapolis, MD 21402, AIAA Member.

<sup>4</sup> Research Associate, Mechanical Engineering Department, 590 Holloway Rd 11/C, Annapolis, MD 21402, AIAA Member.

extraordinary. The inflow condition is not uniform, and must include both the mean shear and the turbulence from the atmospheric boundary layer. Ship motion plays a role – both the change in geometry due to ship pitch and roll, and the linear translation of the ship with respect to the incoming shear flow. The yaw angle of the incoming flow is also variable, and wind gusts are likely to have an important role in the overall dynamics.

Because wind tunnel measurements of a ship airwake pose many of the same challenges, *in situ* data for the validation of ship airwake simulations is required. An ongoing program at the United States Naval Academy uses an instrumented 108-ft (33-m) Navy training vessel, known as a YP, to gather data on the air flow in the near wake of the vessel, above a 18-ft by 22-ft (5.5-m by 6.7-m) stern flight deck. A description of the facility and data for a direct headwind has been discussed previously.<sup>5</sup>

For ship airwake flows, flow topology is known to change drastically with sometimes slight changes in incident wind direction.<sup>4</sup> This necessitates full-field validation data from a number of wind directions, to assess the ability of a simulation to capture changes in flow structure and the particular inflow conditions under which those changes occur. The data presented here is for an inflow that is from 15° to starboard. The flow structure and turbulence levels are quantified, and are compared to the previous data for the direct headwind.

## II. Experiment

A schematic of the experimental facility, YP676, is shown in Fig. 1. The ship is 33-m long, with an aft flight deck and superstructure that resembles an Arleigh Burke Class Destroyer. Air velocity measurements are obtained using three-component sonic anemometers, which measure the full velocity vector at a rate of 20 Hz with minimal instrument interference. Up to eight anemometers may record data simultaneously, with one instrument on the bow at all times to record reference (inflow) conditions. The ship is also equipped with a GPS data logger for measuring ship velocity and position, and an inertial measurement unit (IMU) to record pitch, roll, and yaw.

Velocity measurements are concentrated above the flight deck on the aft end of the ship. Anemometers are mounted on rigid poles at heights ranging from approximately 0.3-m to 2.0-m above the deck. Data acquisition is composed of a series of runs, where the ship is piloted at a constant speed (approx. 8-kts) while maintaining a constant wind-over-deck angle. The wind speed and direction from the bow anemometer are known to the craftmaster in real-time, and are used to maintain heading during a run. Data is collected in the Chesapeake Bay, where the width of the bay and the prevailing winds often allow for runs lasting approximately 30 minutes.

For the data presented here, lengths are nondimensionalized using the step height  $H$  (1.5-m) of the hangar located immediately forward of the flight deck. Velocities are nondimensionalized with the horizontal component of the bow velocity,  $U_\infty$ . The coordinate system has its origin on the ship centerline, on the flight deck, immediately aft of the hangar. The x-direction is aft, y is to starboard, and z is up. Measurement locations in the  $xy$  plane for the current subset of data are shown in Fig. 2. Because of fluctuations in the ambient wind, the raw data must be filtered for both direction and speed. All data where the mean bow velocity is less than 4-m/s is removed, as is all data outside a  $\pm 5^\circ$  window of the target wind-over-deck angle of 15° from starboard.

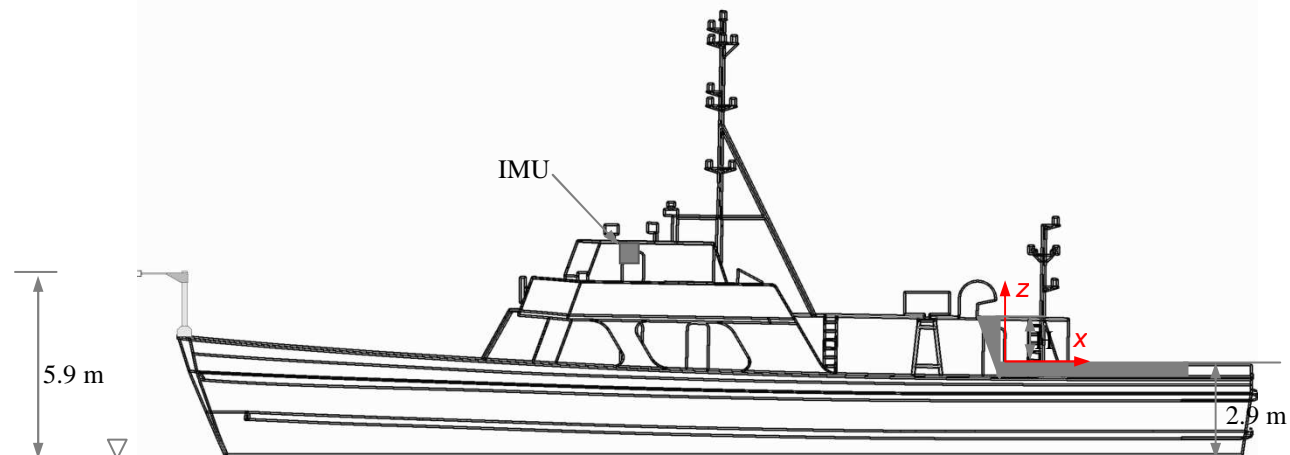


Fig. 1 – Schematic of facility, YP676. Measurements are taken from the aft flight deck, and from a bow anemometer located 5.9 m above the water.

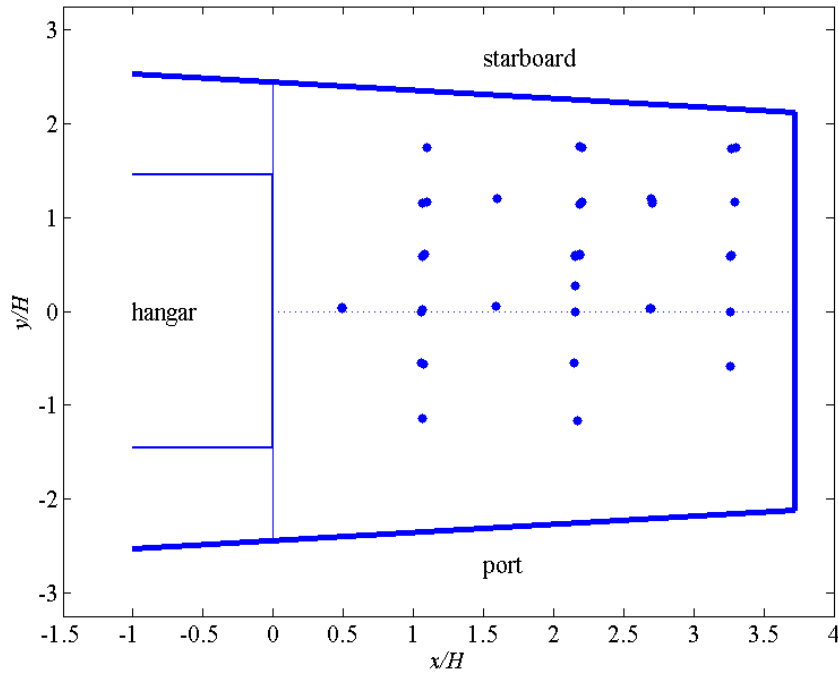


Fig. 2 – Measurement Domain

### III. Results

#### A. Mean Flow

Mean velocities from five cross-sectional profiles over the flight deck are shown in Fig. 3. Multiple arrows at a single point indicate different data runs, generally acquired on different days. Consistency between these data points show qualitatively the repeatability of the experiment. The major wake feature visible from this figure is the recirculation zone, located immediately aft of the hangar. The recirculation is primarily visible in the center plane, (b), and in the two adjacent planes, (a) and (c). This vortex structure is generally the same as that observed in the flow over wall-mounted cubes or prisms, and is also visible in the ship airwake with a direct headwind.<sup>6-8</sup> At an angle of  $0^\circ$  wind-over-deck, the wake flow is symmetrical. The change in wind-over-deck angle from  $0^\circ$  to  $15^\circ$  creates a shift in the position of the vortex, but does not appear to change the overall strength of the structure.

There is a notable change in the sign of the vertical velocity component when comparing velocities at different lateral positions. In planes (c), (d), and (e), there is significant updraft, particularly in the higher end of the measurement domain. A direct comparison between measurements at  $y/H = -0.6$  and at  $y/H = 0.6$  show that this is true for virtually all measured velocities that do not lie directly in the recirculation zone. The downdraft, visible here on the port side of the ship and across the entire flight deck at  $0^\circ$  is presumably due to the low pressure in the wake, again similar to what is seen for wall-mounted cubes or backward-facing step flows. The updraft, therefore, is the result of an additional flow structure that is unique to the ship airwake. Because this is seen on the starboard, upstream side of the ship, it may be a result of the flow moving around the lower hull of the ship and over the edge of the flight deck. Streamlines beginning below the deck height are likely pushed upward, spilling up and over the deck and creating a flow feature not found with a simple headwind. These streamlines would have a very different history than those coming from over the upper ship superstructure, and therefore the wake turbulence in this region may also be qualitatively different.

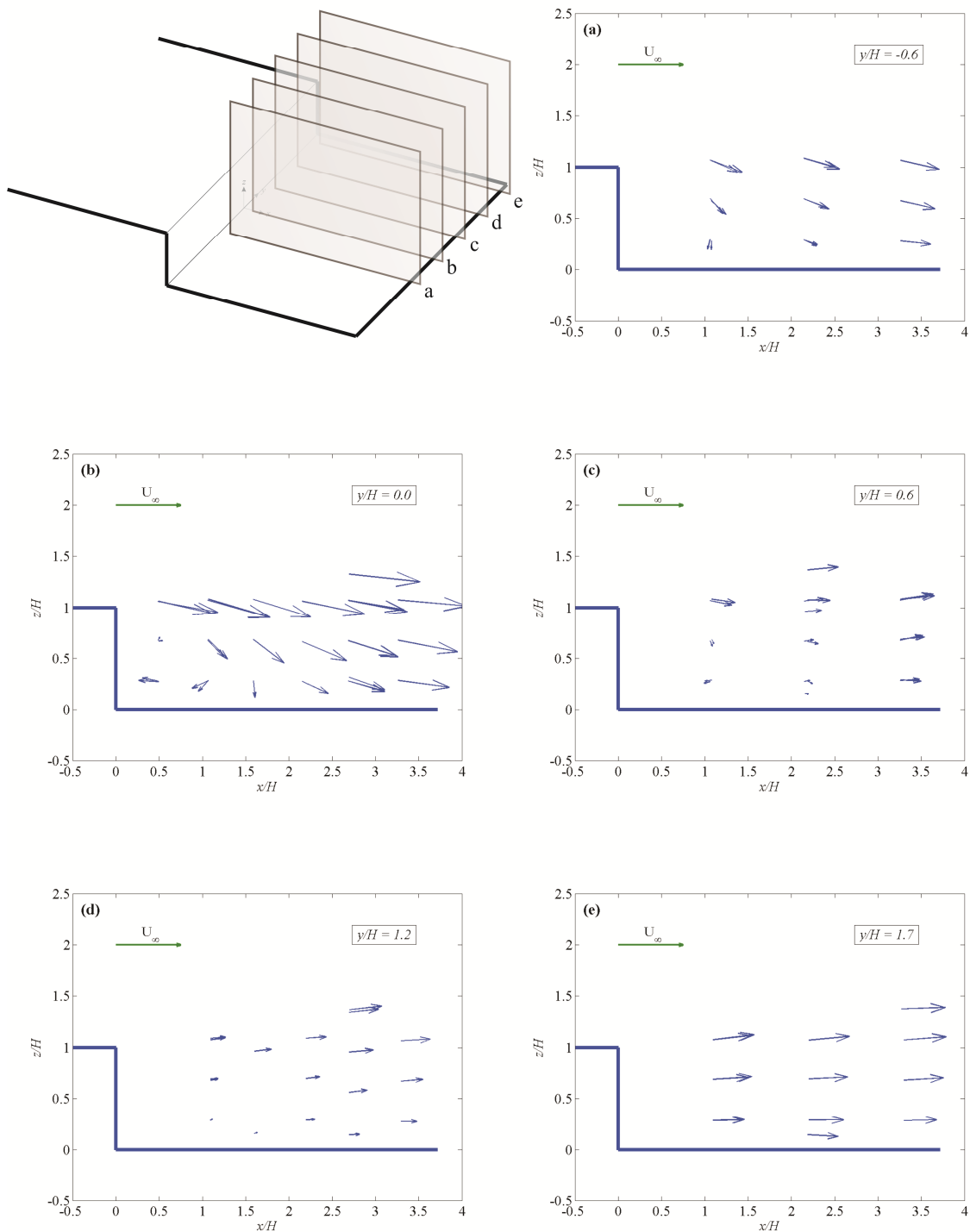


Fig. 3 – Mean velocity profiles at five sections over the flight deck. Note the lack of symmetry between sections (a) and (c).

Figure 4 shows the mean velocity profile in the  $yz$  plane, at a distance  $x/H = 1.1$  from the hangar structure. This is the view one would see standing on the stern of the ship, looking forward, at a cross-section which sits within the primary recirculation. From this perspective the updraft over the starboard side of the deck is clear, as is the resulting mean shear. In the symmetric case two counter-rotating vortices are expected, while one large vortex is visible here. It is unclear whether a second, smaller vortex is present on the port side, since no measurements are available for that region.

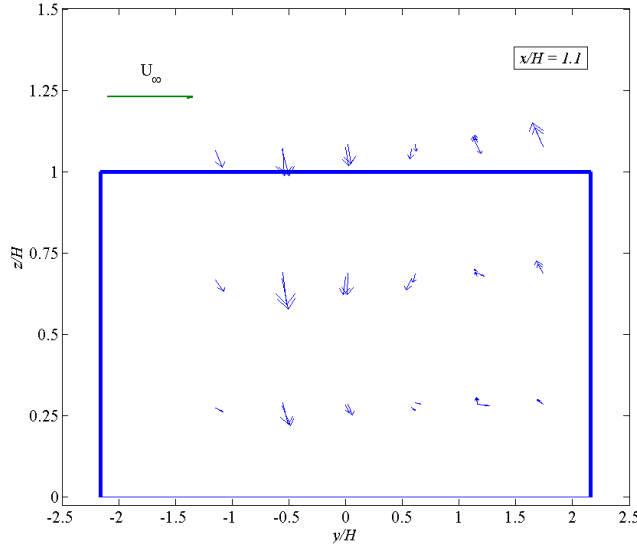


Fig. 4 – Mean velocity in the  $yz$  plane.

## B. Turbulent Stresses

An understanding of the flow turbulence in the ship airwake is required for the estimation of the fluctuating loads on an immersed rotorcraft, and therefore the pilot workload. One of the most useful descriptions of the turbulent fluctuations is the Reynolds stress, defined as

$$R_{ij} = \overline{u_i u_j} / U_\infty^2$$

where  $U_\infty$  is the horizontal component of the bow velocity,  $u_i$  is the fluctuating part of the local velocity, and the overbar denotes averaging. The normal Reynolds stress,  $R_{uu}$ , along the ship centerline at various points above the flight deck is shown in Fig. 5. Figures 7 and 9 show the Reynolds shear stress,  $R_{uw}$ , and the turbulent intensity,  $u'/U$ , respectively. For comparison purposes, the same quantities for the case of a direct headwind ( $\beta = 0$ ) are shown in Figs 6, 8, and 10.

From Fig. 5, the normal stress component along the ship, there is a clear trend of increasing stress with increased height above the flight deck. This appears to be true for both points that are still within the main recirculation region, as in Fig. 5a, and for points that are clearly downstream of the primary structure, in Fig 5c-d. Compared to the same measure at the same locations with an inflow condition of  $\beta = 0$  (Fig. 6), the normal stresses are larger significantly larger in the cross-wind case. One possible explanation for this is that much of the fluctuation in  $u$  is due to atmospheric turbulence (some of which is at very large scales), and less is due to the wake turbulence. In the cross-wind case, the measurement regions have greater exposure to the inflow, meaning that the ship superstructure has had less opportunity to break up the large eddies that result in measurement of large  $R_{uu}$ .

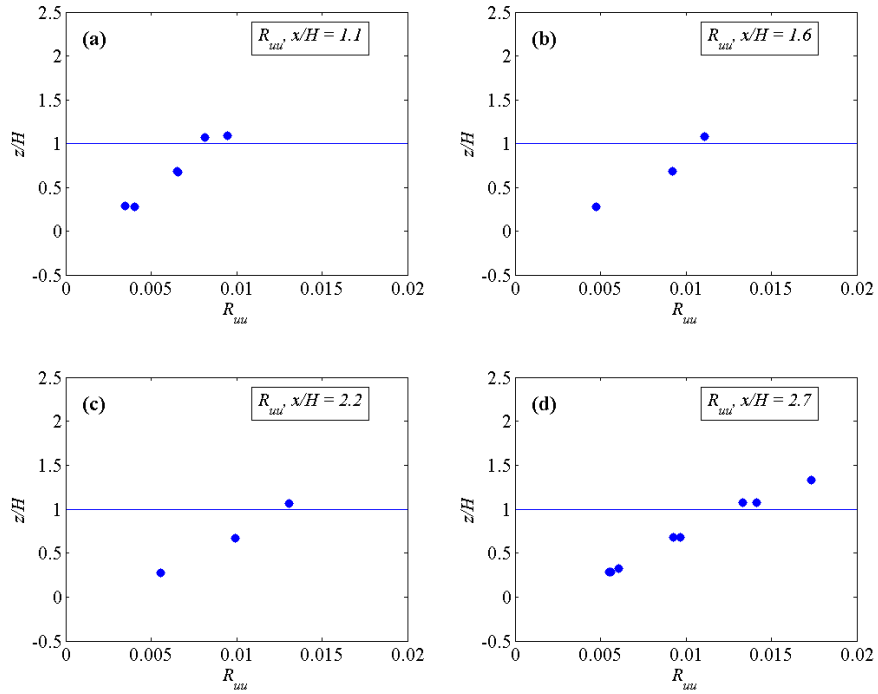


Fig. 5 – Normal, streamwise Reynolds stress over the flight deck, along the ship centerline. Data is for cross-wind case; compare to Fig. 6, showing the same quantity for a direct headwind.

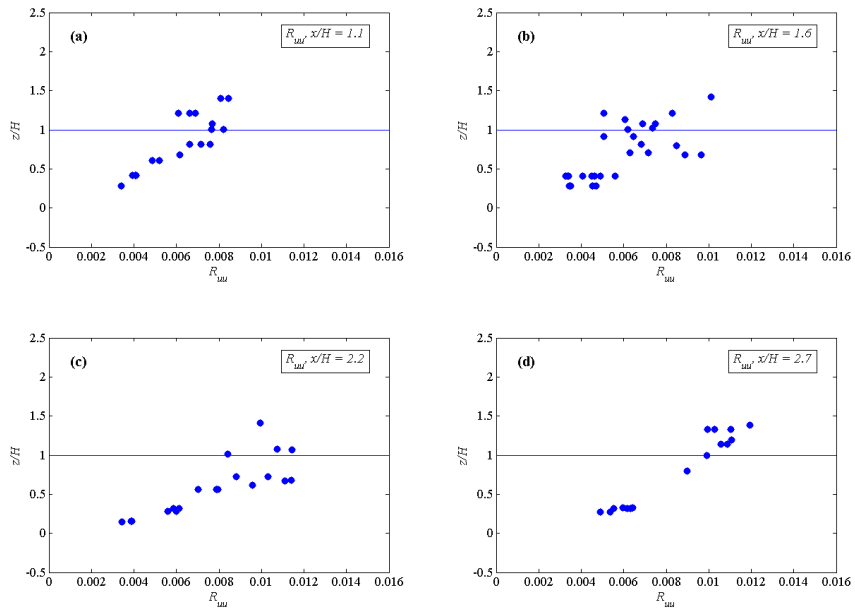


Fig. 6 – Normal, streamwise Reynolds stress along the ship centerline for the case of a direct headwind, from Brownell et al.<sup>5</sup>

Figures 7 and 8 show the Reynolds shear stress,  $R_{uw}$ , plotted at various heights along the centerline for both  $\beta = 15$  and  $\beta = 0$  winds. Reynolds shear stresses are known to be associated with the presence of turbulent structures and can be revealing when exploring the topology of a new flow. For both inflow conditions, the max shear stresses are found at an intermediate height for all positions except for the farthest downstream. This is in contrast to the normal stresses, which increased with  $z/H$  throughout the entire measurement domain. A specific height for the peak shear stress cannot be determined due to a lack of spatial resolution, but the current measurements tend to mirror those from  $\beta = 0$ , for which many more data points are available and the peak height was determined to be approximately  $z/H = 0.7$ . From wind tunnel measurements over a ship superstructure (without a simulated boundary layer), other researchers have observed the same trends in  $R_{uw}$ .<sup>6</sup> In terms of magnitude, the shear stress appears to be similar for points at a given height for the three planes nearest the hangar step. For the farthest plane, magnitudes below the hangar height are similar while the shear stress above the hangar is considerably larger. These trends are also the same for both inflow conditions, and unlike the  $R_{uu}$  values, there is no clear difference in magnitude as a result of inflow direction. The reason for large  $R_{uw}$  at the highest levels in Fig. 7d is likely due to vortex structures shed from the upstream ship superstructure, although it may also be influenced by the updraft coming over the flight deck from below. Compared to the headwind case, much more vorticity is likely formed along the starboard edge of the flight deck. This turbulence would be advected downstream and across the deck, and should be measurable at higher values of  $x/H$ . To the extent of the current data, the shear stresses at the most downstream positions appear slightly larger in the crosswind case than in the headwind case, but this cannot be determined with certainty.

The turbulence intensity, defined as the average of the root-mean-square of the component velocity fluctuations normalized by the mean velocity, is displayed in Fig. 9 for the crosswind case and in Fig. 10 for the headwind case. The turbulence intensity appears structurally similar to the normal Reynolds stress  $R_{uu}$ , which is not surprising considering that is the stress component with the greatest magnitude. There is also little difference when comparing the turbulence intensity for the two wind directions. The trends appear to be identical, and the difference in magnitudes, if any, is slight. This data perhaps raises the point that, as an averaged quantity, the turbulence intensity is not as useful for understanding the flow (or the effect of the flow on a helicopter) as the individual stress components. The turbulence intensity and the related turbulent kinetic energy (TKE) give an estimate of the magnitude of fluctuations, but lose information on isotropy and on the potential sources of the turbulence. For the purposes of helicopter flight, regions of the flow with high turbulence intensity may not be as challenging for flight operations as regions with lower intensity turbulence but more turbulent shear.

### C. Analysis of large scales

To better understand the effects of the large flow scales, two-point cross-correlations are computed between the bow anemometer and the anemometers on the flight deck. The cross-correlation,  $\rho_{ij}(t)$ , as a function of lag time  $t$  is computed as:

$$c_{ij}(t) = \begin{cases} \frac{1}{n} \sum_{\tau=1}^{n-t} (i_{\tau} - \bar{i})(j_{\tau+t} - \bar{j}) & t = 0, 1, 2, \dots \\ \frac{1}{n} \sum_{\tau=1}^{n+t} (j_{\tau} - \bar{j})(i_{\tau-t} - \bar{i}) & t = 0, -1, -2, \dots \end{cases}$$

$$\rho_{ij}(t) = \frac{c_{ij}(t)}{\sqrt{c_{ii}(0)}\sqrt{c_{jj}(0)}}$$

where  $i$  is a bow velocity component,  $j$  is the corresponding wake velocity component, and  $\tau$  is the record time. For the data shown in Fig. 11, this is computed between the bow anemometer, located at  $x/H = -18.953$ , and an anemometer over the flight deck. For all three figures, the cross-correlation function between the bow and all anemometers in a given bin are averaged to provide the result shown. For Fig. 11a, the bin is  $0.9 < x/H < 1.3$ ,  $y/H > 1.0$ , and  $z/H > 0.5$ . For Figs. 11b and 11c the range in  $x/H$  changes to  $2.0 < x/H < 2.4$  and  $3.1 < x/H < 3.5$ , respectively, while the restrictions in  $y$  and  $z$  are unchanged. Simply, the figures show the correlation between velocities at the bow and velocities at three different positions within the wake, with those positions each located on the starboard side of the ship and at least one half hangar height above the deck.

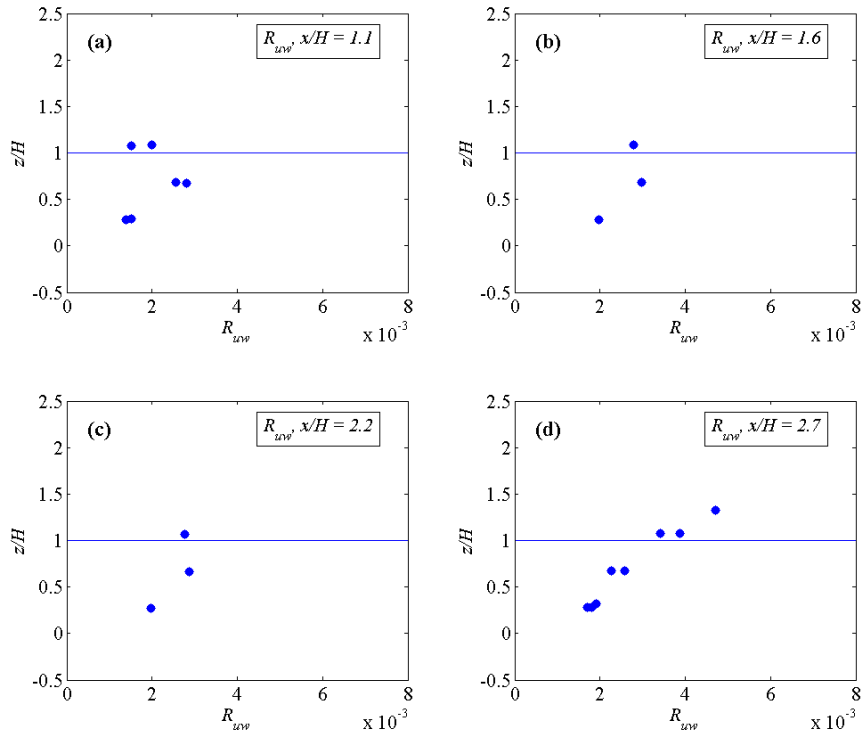


Fig. 7 – Reynolds shear stresses, measured at various locations over the flight deck, along the ship centerline. Data is for a crosswind of  $\beta = 15$ ; compare to Fig. 8, showing same data for a headwind.

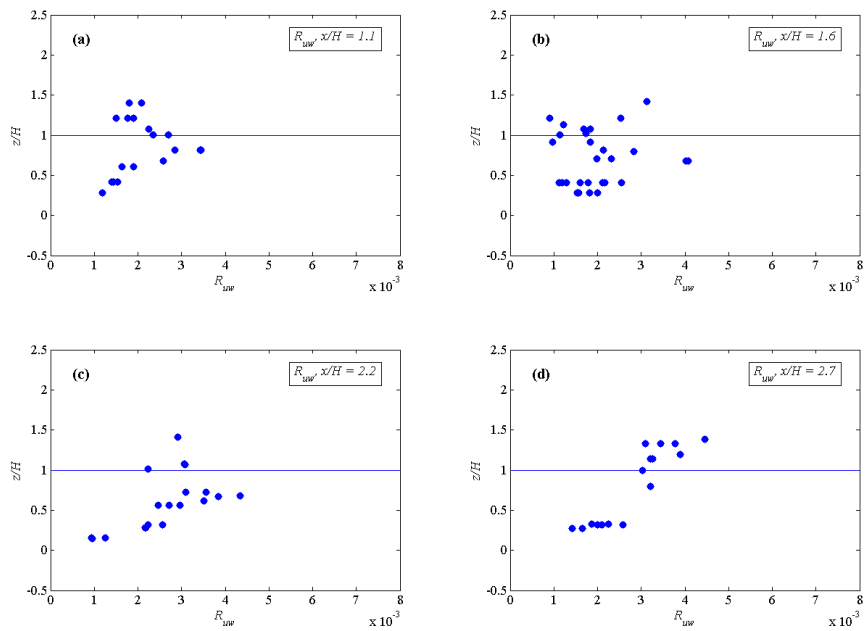


Fig. 8 – Shear stress over the flight deck with a headwind, from Brownell et al.<sup>5</sup>

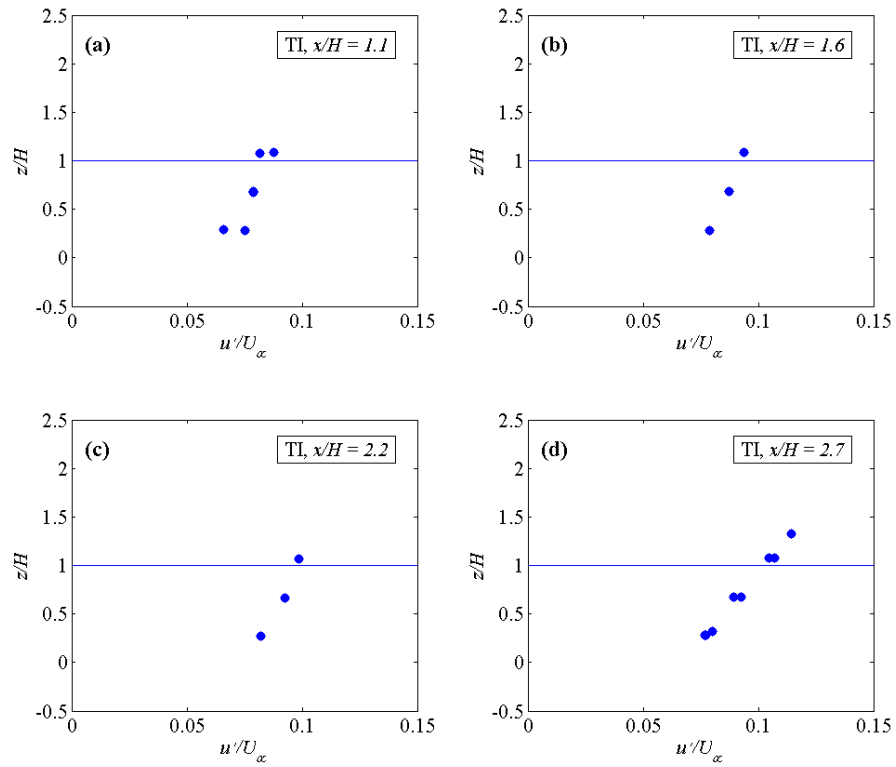


Fig. 9 – Turbulent intensity, measured at various locations over the flight deck, along the ship centerline. Data is for a crosswind of  $\beta = 15$ ; compare to Fig. 10, showing same data for a headwind.

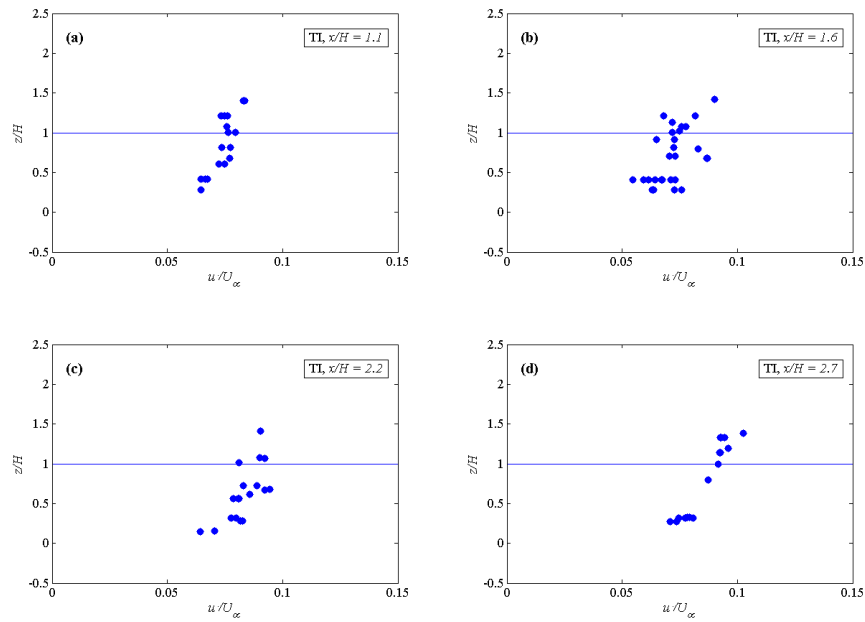


Fig. 10 – Turbulence intensity for  $\beta = 0$ , from Brownell et al.<sup>5</sup>

In the figures, lag time has been normalized as  $t^* = tU_\infty/L$ , where  $U_\infty$  is the mean bow velocity in the  $x$ -direction, approximately 7.8 m/s, and  $L$  is the distance between bow and wake anemometers, which varies from approx. 30 m to 33 m. If the bow velocity is the appropriate large-scale advective velocity for the flow, one would then expect to see a correlation between bow and wake velocities at a lag time of  $t = L/U_\infty$ , the time it takes for a turbulent eddy to translate downstream a distance  $L$ . For clarity, a vertical line has been added to each of the three plots in Fig. 11 at  $t^* = tU_\infty/L = 1$ .

From the figure, correlations in the  $v$  and  $w$  velocity components, particularly those in the far wake, display the shape expected considering the assumed advective velocity. The correlation functions have minimal skewness, and have a clear peak at  $t^* = 1$ . An alternative view of this result is that it provides a confirmation that the velocity as measured by the bow anemometer is the appropriate velocity for scaling measurements in the wake. If, for example, the measurements from the bow were already significantly disturbed by the presence of the ship, then there would be no reason for any of the correlation functions to show a peak at  $t^* = 1$ .

Compared to the correlations in  $v$  and  $w$ , the correlations in  $u$  have a very different shape and different peak lag time. For all three deck positions, the correlations in  $u$  show a delayed peak with very little correlation until at least  $t^* = 1$ . The correlation functions then rise rapidly, and taper to a broad peak centered around  $t^* = 2.2$ . The overall function has significant positive skewness, which contrasts sharply with the  $v$  and  $w$  correlations.

Several explanations for the behavior of the correlation function in  $u$  have been considered. First, the  $u$  component of velocity is by far the largest on average, and eddies due to atmospheric turbulence are much larger in the horizontal plane than in the vertical plane. While velocity changes in  $w$ , and to a certain extent in  $v$ , are due to turbulent eddies,  $u$  is more susceptible to large, low-frequency fluctuations in the wind speed. This may explain the breadth of the peak, but it does not address the particular shape or position of the correlation function. For a flow with a fluctuating mean velocity, there are presumably as many points where the local mean is greater than the sample mean as when it is less. A greater local mean velocity would cause eddies to reach the deck anemometer(s) faster than expected, and would result in greater correlation over the range  $0 < t^* < 1$ . This result is not found in the data.

A more likely explanation for the increased correlation lag time is the velocity deficit in the wake of the ship. Because the bow anemometer is not influenced by the presence of the ship, the cross-correlation is meant to be a measure of atmospheric turbulence, largely unaffected by details of the wake. If the inflow were entirely uniform, there would be no correlation in any of the velocity components. However, the effect of the wake is obviously to decrease the local mean velocity, and for eddies that travel in a straight line between the anemometers, the transit time is likely not determined by the simple function above. These eddies, traveling in this direction, would have a large  $u$  velocity component (relative to the other components) and would therefore have a much greater effect on  $\rho_{uu}$  than on anything else.

Interestingly, ship motion plays a small role. Although it is not clear from the figures included here, there is a small but distinct peak in the correlation function at  $tU_\infty/L = 0$  for all velocity components and at all deck locations. Because the anemometers are all mounted to the same rigid platform, this can only be due to ship motion effects.

#### IV. Conclusions

Velocity measurements in the wake of a US Navy surface ship have been presented for an inflow condition of  $15^\circ$  to starboard. The bulk of the measurements are taken above an aft flight deck, and in this region the flow shows a distinct mean structure. An asymmetric recirculation zone sits immediately behind the aft hangar. The primary recirculation is strongly influenced by an updraft from the starboard side, presumably due to the air flowing up and over the starboard edge of the deck. This asymmetry was not observed in measurements of the flow with a direct headwind.

Turbulence statistics in the form of Reynolds stresses are presented for points along the ship centerline. It is observed that, compared to the case of a direct headwind, the normal stress  $R_{uu}$  is larger with the crosswind while the shear stress and the overall turbulent intensity are mostly unchanged. The increase in the measured normal stress is possibly due to increased exposure to atmospheric turbulence, i.e. the apparent ship superstructure for a crosswind may be viewed as either smaller or more streamlined compared to what the flow sees with a headwind.

Velocity correlations between bow and wake anemometers are used to assess the large scales of the flow. Significant differences are observed depending on which velocity component is correlated, smaller differences are observed depending on which wake anemometers are included in the correlation.

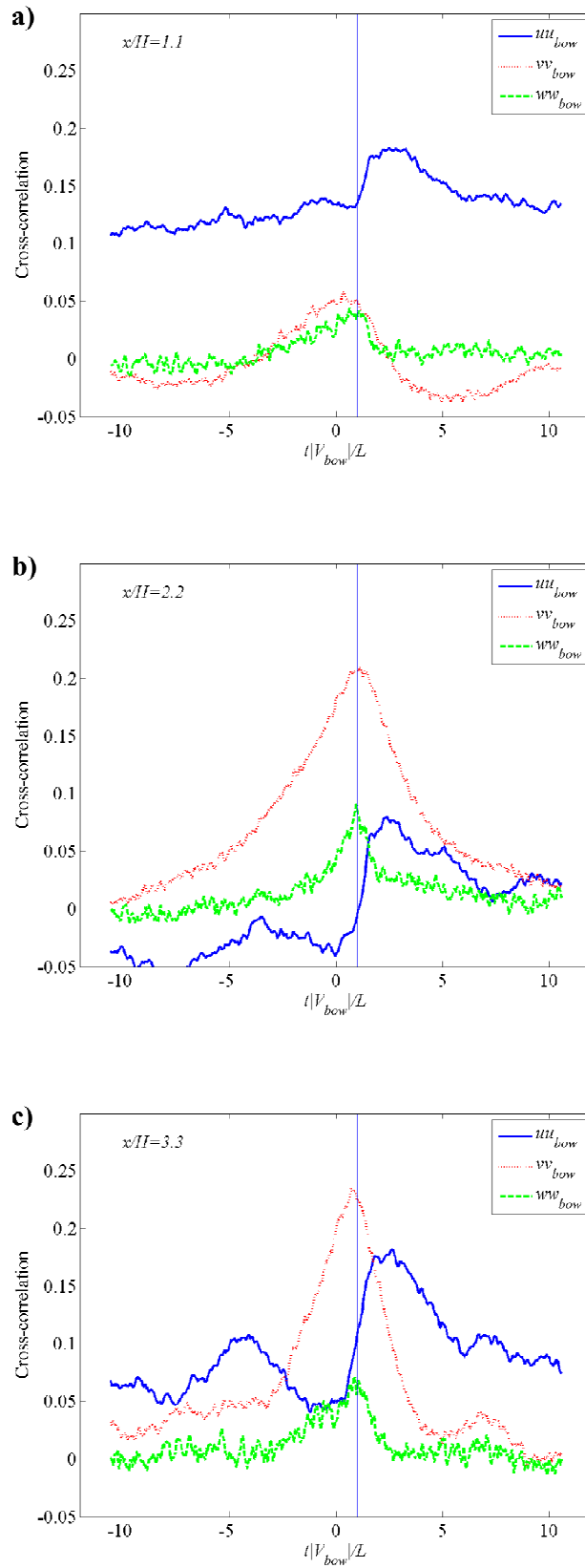


Fig. 11 – Bow-wake correlation at  $x/H = 1.1, 2.2,$  and  $3.3$ .

## Acknowledgments

Support from the Office of Naval Research Young Investigator Program (PI: MR Snyder) is gratefully acknowledged. The authors would also like to recognize assistance from Colin Wilkinson, John Burks, and Joshua Shishkoff.

## References

- <sup>1</sup> Sezer-Uzol, N., Sharma, A., and Long, L.N., "Computational fluid dynamics simulations of the ship airwake," *Proceedings of the Institution of Mechanical Engineers*, vol. 219, no. 5, 2005.
- <sup>2</sup> Polsky, S., Imber, R., Czerwicz, R., and Ghee, T., "A computational and experimental determination of the airflow around the landing deck of a US Navy Destroyer (DDG): Part II," in *AIAA Fluid Dynamics Conference and Exhibit*, 2007.
- <sup>3</sup> Forrest, J.S., and Owen, I., "An investigation of ship airwakes using Detached-Eddy Simulation," *Computers & Fluids*, vol 39, no. 4, 2010.
- <sup>4</sup> Zan, S.J., "On aerodynamic modeling and simulation of the dynamic interface," *Proceedings of the Institution of Mechanical Engineers*, vol. 219, no. 5, 2005.
- <sup>5</sup> Brownell, C.J., Luznik, L., Snyder, M.R., Kang, H.S., and Wilkinson, C.H., "In situ velocity measurements in the near wake of a ship superstructure," *Journal of Aircraft*, forthcoming.
- <sup>6</sup> Tinney, C.E., and Ukeiley, L.S., "A study of a 3D double backward-facing step," *Experiments in Fluids*, vol 47, 2009.
- <sup>7</sup> Uffinger, T., Becker, S., and Ali, I., "Vortex dynamics in the wake of wall-mounted cylinders: experiment and simulation," 15<sup>th</sup> International Symposium on Applications of Laser Techniques to Fluid Mechanics, Lisbon, Portugal, July 2010.
- <sup>8</sup> Castro, I.P., and Robins, A.G., "The flow around a surface-mounted cube in uniform and turbulent streams," *Journal of Fluid Mechanics*, vol 79, no. 2, 1977.